

# Exploring the Origin of the Ion Selectivity of the KcsA Potassium Channel

Anton Burykin, Mitsunori Kato, and Arieh Warshel\*

Department of Chemistry, University of Southern California, Los Angeles, California

**ABSTRACT** The availability of structural information about biological ion channels provides an opportunity to gain a detailed understanding of the control of ion selectivity by biological systems. However, accomplishing this task by computer simulation approaches is very challenging. First, although the activation barriers for ion transport can be evaluated by microscopic simulations, it is hard to obtain accurate results by such approaches. Second, the selectivity is related to the actual ion current and not directly to the individual activation barriers. Thus, it is essential to simulate the ion currents and this cannot be accomplished at present by microscopic MD approaches. In order to address this challenge, we developed and refined an approach capable of evaluating ion current while still reflecting the realistic features of the given channel. Our method involves generation of semimacroscopic free energy surfaces for the channel/ions system and Brownian dynamics (BD) simulations of the corresponding ion current. In contrast to most alternative macroscopic models, our approach is able to reproduce the difference between the free energy surfaces of different ions and thus to address the selectivity problem. Our method is used in a study of the selectivity of the KcsA channel toward the  $K^+$  and  $Na^+$  ions. The BD simulations with the calculated free energy profiles produce an appreciable selectivity. To the best of our knowledge, this is the first time that the trend in the selectivity in the ion current is produced by a computer simulation approach. Nevertheless, the calculated selectivity is still smaller than its experimental estimate. Recognizing that the calculated profiles are not perfect, we examine how changes in these profiles can account for the observed selectivity. It is found that the origin of the selectivity is more complex than generally assumed. The observed selectivity can be reproduced by increasing the barrier at the exit and the entrance of the selectivity filter, but the necessary changes in the barrier approach the limit of the error in the PDL/D-S-LRA calculations. Other options that can increase the selectivity are also considered, including the difference between the  $Na^+ \cdots Na^+$  and  $K^+ \cdots K^+$  interaction. However, this interesting effect does not appear to lead to a major difference in selectivity since the  $Na^+$  ions at the limit of strong interaction tend to move in a less concerted way than the  $K^+$  ions. Changes in the

relative binding energies at the different binding sites are also not so effective in changing the selectivity. Finally, it is pointed out that using the calculated profiles as a starting point and forcing the model to satisfy different experimentally based constraints, should eventually provide more detailed understanding of the different complex factors involved in ion selectivity of biological channels. *Proteins* 2003;52:412–426. © 2003 Wiley-Liss, Inc.

**Key words:** ion current; protein electrostatics; dielectrics; ion channels; selectivity

## INTRODUCTION

The control of ion permeation by transmembrane channels underlies many important biological functions (e.g., Ref. 1). Electrophysiological studies have provided crucial information about the overall transport process and about some of its important details (e.g., Refs. 1–3). Recent structural studies of the  $K^+$  channel (KcsA from *Streptomyces lividans*<sup>4,5</sup>) coupled with other experimental information have revolutionized the field by offering the opportunity to understand the nature of biological ion transport on a molecular level.

Despite the above progress, there are important issues that have not been resolved on a satisfactory microscopic level. One of the key problems is the nature of the selectivity of ion channels toward different ions. For example, the KcsA channel allows  $K^+$  ions to pass with an optimal efficiency while restricting the transport of  $Na^+$  ions by a large factor (this factor is thought to be about 1,000,<sup>6</sup> although some studies estimated this factor to be lower<sup>7</sup>). While reasonable proposals for the origin of this selectivity are available,<sup>5,8–11</sup> it is still unclear what are the exact factors that control this crucial process (see below). Thus, it is quite clear that some form of computer-based structure-function correlation is essential for a quantitative resolution of the selectivity problem.

Despite the progress in modeling of ion channels (e.g.,<sup>8–10,12–20</sup>), development of a practical and reliable

---

Grant sponsor: National Institute of Health; Grant number: GM40283.

\*Correspondence to: Arieh Warshel, Department of Chemistry, University of Southern California, 3620 McClintock Ave., SGM 418, University Park Campus, Los Angeles, CA 90089-1062. E-mail: warshel@usc.edu

Received 19 December 2002; Accepted 21 February 2003

approach is still extremely challenging. That is, although some workers might view the present situation with regards to selectivity calculations as a reasonable stage,<sup>17</sup> the situation is far from satisfactory for the KcsA channel. Computer simulation approaches that involve free energy perturbation mutations of  $K^+$  to  $Na^+$  have given very different results depending on the parameters used and the treatment of long range effects. Allen et al.<sup>18</sup> obtained a difference of about 12 kcal/mol between the highest barriers for  $Na^+$  and  $K^+$ . A more systematic study of this group<sup>9</sup> gave a difference of 5.4 kcal/mol at the outer side of the selectivity filter. Biggin et al.<sup>21</sup> obtained a difference of about 20 kcal/mol between the energy profiles of  $Na^+$  and  $K^+$  in the filter region and larger difference in the gate region. Another study<sup>19</sup> reported a difference in the free energy of mutating  $K^+$  to  $Na^+$  in the first and second loading sites of 2.8 and 6.6 kcal/mol, respectively. However, although this study evaluated the activation barrier for the concerted motion of  $K^+$  ions, it did not consider the differences between the activation barriers of the  $K^+$  and  $Na^+$  ions. At any rate, none of the above studies reported the selectivity for a simultaneous transfer of two or more ions, which is thought (e.g.,<sup>5</sup>) to be involved in the actual conduction process. The study of Luzhkov and Aqvist,<sup>8</sup> which used perhaps the most reliable computational model, gave a relatively small free energy difference (about 2 kcal/mol) for mutating a single  $K^+$  to a single  $Na^+$  at the minima of the loading states and a larger difference (up to 4 kcal/mol) for mutating two  $K^+$  to two  $Na^+$  at the minima of the loading states. This study provided feasible hints for the origin of the selectivity and an earlier study of these workers<sup>16</sup> evaluated the barrier for a concerted motion of  $K^+$  ions. However, the difference between the free energies of the  $K^+$  and  $Na^+$  ions were not evaluated at the barriers' regions. Furthermore, all of the above free energy calculations did not involve current calculations and thus could not determine what selectivity would be obtained with the calculated energetics. Another interesting attempt to explore the selectivity problem was reported by Shrivastava et al.<sup>10</sup> These researchers found by direct MD simulation that the  $K^+$  ion moves between neighboring sites during the simulation time, while the  $Na^+$  ion does not move during that time ( $\sim 2$  ns). Unfortunately, it was not possible to determine how long it would take for the  $Na^+$  ion to move, nor what the current will be at a given ion concentration. Other problems might be associated with the overall reliability of microscopic calculations of the free energy profile of  $K^+$  or  $Na^+$  (see discussion in Burykin et al.<sup>20</sup>).

It seems to us that the issue of ion selectivity cannot be resolved quantitatively or even qualitatively without calculating the corresponding ion current, which is the actual direct observable in the system. Such a calculation should be able to convert the free energy profile of the system to the corresponding time dependence of the ion permeation process.

The present work conducts a systematic study of the origin of the  $K^+/Na^+$  selectivity in the KcsA channel. Our approach focuses on calculations of the actual ion current,

while trying to use as much as possible information from semimicroscopic and microscopic calculations of the free energy surfaces for a single ion and two-ions transport, as well as on the corresponding effective friction. In other words, we follow our recently developed approach<sup>20</sup> where we attempt to use state-of-the-art calculations of the energetics and dynamics of one and two ions and then to "map" our finding on a more simplified channel model where we can use Langevin Dynamics (LD) simulations to explore the ion current. Conceptually this approach is similar to the approach used by Chung and coworkers,<sup>22</sup> but the crucial difference is in the emphasis on a realistic and complete treatment of the electrostatic problem, which is very critical in the present case (see Concluding Remarks). In fact, the present approach is most similar conceptually to the approach used in our simulations of proton translocations in proteins.<sup>23</sup>

The use of a micro-macro approach helps us to reduce the wide range of feasible options for the origin of selectivity. We are able to reproduce a part of the overall selectivity of the KcsA channel without any arbitrary parameterization and then to explore in a systematic way factors that can account for the overall selectivity.

## SIMULATION METHODS

Our aim is to evaluate the ion current in a realistic model of the KcsA channel and to try to reproduce the observed selectivity. This challenging task cannot be accomplished at present by direct MD simulations. Thus, we have to find a compromise that captures the key features of the system while still allowing for simulations of long time processes. Our strategy of accomplishing this task has been described recently in great details,<sup>20</sup> but here we introduce several important improvements and modifications that will be considered below.

Our calculations of ion current are based on evaluating the motion of the ions by a Langevin equation<sup>24</sup>:

$$m_i \ddot{r}_{i\alpha} = -m_i \gamma_i \dot{r}_{i\alpha} - \partial \Delta G / \partial r_{i\alpha} + A_{i\alpha}(t) - \partial \Delta G_{\text{ext}} / \partial r_{i\alpha} \quad (1)$$

where  $i$  runs over the ions,  $\alpha$  runs over the  $x$ ,  $y$ , and  $z$  Cartesian coordinates of each ion,  $m_i$  is the mass of the  $i$ th ion,  $\gamma_i$  is the friction coefficient for the  $i$ th ion, and  $A_{i\alpha}$  is a random force, which is related to  $\gamma_i$  through the fluctuation-dissipation theorem.<sup>25</sup> The free energy  $\Delta G_{\text{ext}}$  represents the effect of the external electric field (see below). The use of Eq. (1) in simulation of ion current is not new (see Chung et al.<sup>22</sup>). What is new and in some respects unique to our approach is the insistence on obtaining an as reliable as possible description of the free energy surface  $\Delta G(r)$  from semimacroscopic and/or microscopic simulations. Our treatment describes the total electrostatic free energy of the ions in the system by

$$\Delta G(r) = \sum_i \Delta \Delta G_i(\mathbf{r}_i) + \sum_{i>j} \Delta G_{ij}(\mathbf{r}_{ij}) + \sum_{i,k} \Delta G_{ik}(\mathbf{r}_i, \mathbf{R}_k) \quad (2)$$

where  $r$  and  $R$  represent, respectively, the coordinates of the ions and the ionizable residues of the protein. Here  $\Delta \Delta G_i(\mathbf{r}_i)$  is the free energy invested in moving a single ion from water to the specific position in the channel,  $\mathbf{r}_i$  The

notation  $\Delta\Delta G$  is used because  $\Delta G$  corresponds to the process of moving the ion from water to its channel site, and our calculations involve an exchange of a single water molecule by the ion. That is, the ion penetration leads in most cases to a displacement of a water molecule, which is equivalent in a thermodynamic sense to a transfer of this molecule to the bulk solvent (more dynamical aspects of this effect are also considered). The overall  $\Delta\Delta G_i$  term is expressed as

$$\Delta\Delta G_i(\mathbf{r}_i) = \Delta\Delta G_{\text{self}}(0, 0, z_i) + \Delta\Delta G_{\text{steric}}(x_i, y_i, z_i) \quad (3)$$

where  $\Delta\Delta G_{\text{self}}$  is the electrostatic self energy of the ion and  $\Delta\Delta G_{\text{steric}}$  is the steric interaction between the ion and the channel (see below).

In evaluating  $\Delta\Delta G_i$  for a specific ion one may try to use a fully microscopic FEP approach<sup>26</sup> or a semimacroscopic approach such as the PDL/D/S-LRA approach (e.g., Ref. 27). At present, we believe that for ions in the interior of the KcsA channel one obtains more reliable results with semimacroscopic approaches (see discussion in Burykin et al.<sup>20</sup>). However, here we also consider microscopic results for the free energies of mutating  $K^+$  to  $Na^+$ . Here, we use the fact that FEP calculations for “mutations” are quite reliable and sometimes sufficiently stable to replace the semimacroscopic results (note that this is not the case for calculations of the absolute  $\Delta\Delta G_i$ ).

The ion-ion interaction term  $\Delta G_{ij}$  is represented as in our previous work<sup>20</sup> by

$$\Delta G_{ij} = 332\bar{q}_i\bar{q}_j/(r_{ij}\epsilon_{\text{eff}}(r_{ij})) + \Delta G'(r_{ij}) \quad (4)$$

where  $\bar{q}_i$  and  $\bar{q}_j$  are the charges of the corresponding ions and  $\epsilon_{\text{eff}}(r)$  is a dielectric function, which is given by:

$$\epsilon_{\text{eff}}(r) = 1 + \epsilon'(1 - \exp(-\bar{a}r)) \quad (5)$$

This type of function has been shown<sup>27–29</sup> to provide the consensus of experimental and theoretical studies of charge-charge interactions in proteins. Using for  $\bar{a}$  values between 0.1 to 0.18 tends to give good results in proteins.<sup>27</sup> There we used  $\bar{a} = 0.15$  and examined the effect of  $\epsilon'$ . The  $\Delta G'(r_{ij})$  term is an additional interaction potential that will be discussed below. The validity of the first term in Eq. (4) and its excellent performance has been repeatedly illustrated (e.g., Ref. 27) and one way to clarify this point is to emphasize that the use of this equation is physically equivalent to the use of the highly popular Generalized Born’s equation (see discussion in Warshel and Papazyan<sup>30</sup>). Finally, we would like to emphasize that the validity of our assumption that  $\epsilon_{\text{eff}}$  is large has been demonstrated in Burykin et al.<sup>20</sup> by explicit calculations.

Another way to look at the first term of equation (4) is to view it as a tool for interpolating the calculated results for ion-ion interaction to the general effective potential of Eq. (3). In doing so, we have to keep in mind that present microscopic calculations do not provide the full solvation compensation for the change in ion-ion interaction in charge separation processes.<sup>28</sup> Thus the  $\epsilon_{\text{eff}}$  obtained from microscopic calculations frequently overestimates the corresponding  $\epsilon_{\text{eff}}$  obtained from experimental analysis.

The second term in Eq. (4) (the  $\Delta G'$  term) is given by

$$\Delta G'(r_{ij}) = Ar^{-8} + K_{\text{filter}}(z_{ij} - z_{ij}^o)^2 \quad (6)$$

The first term represents a simple steric repulsive term between the ions. This term prevents ions of opposite sign from “collapsing” together. Using  $A = 1,525 \text{ kcal}\cdot\text{mol}^{-1}\cdot\text{\AA}^8$  kept the  $K^+ Cl^-$  and  $Na^+ Cl^-$  ion pairs at an equilibrium distance of about 3 Å in water ( $\epsilon = 80.0$ ). This term has no effect on the relevant interaction between ions of the same sign such ion pairs do not reach a very close distance.

Since the second term has a much more complex origin. That is, when two ions enter a narrow channel they tend to keep the same number of water molecules between them. Thus, if the  $i$ th ion enters the channel first and the  $j$ th ion follows, with one water molecule between them, increasing the separation between the ions will lead to an empty space and the energy of the system will increase (relative to the situation where water molecules are allowed to feel any empty space). Since we deal with an implicit model without explicit water molecules, we account for this effect by the second term of Eq. (6). This term is implemented with the following protocol. We start by setting  $K_{\text{filter}}$  to zero and leave it zero as long as one of the ions is out of the filter. In the first time that both ions are in the filter, we set  $K_{\text{filter}} = 1.0 \text{ kcal/mol}$  and take  $z_{ij}^o = 7.0 \text{ \AA}$ . Other alternative values of  $K_{\text{filter}}$  are also examined. Note that this term is similar in nature to the term used by Edwards et al.<sup>31</sup>

The  $\Delta\Delta G_{\text{steric}}$  term of Eq. (3) is obtained by modifying our previous treatment and moving from an explicit ion-protein steric interaction to a simplified half-quadratic potential of the form

$$\Delta G_{\text{steric}}^{\text{channel}}(x_i, y_i, z_i) = \begin{cases} K_{\text{steric}} \cdot (\xi_i - \xi_o(z_i))^2, & \xi_i \geq \xi_o(z_i) \\ 0, & \xi_i < \xi_o(z_i) \end{cases} \quad (7)$$

where  $\xi_i^2 = x_i^2 + y_i^2$  and  $K_{\text{steric}}$  is a force constant. For the interface between the boundaries of the membrane/protein system and the bulk solution, we also used a half-quadratic potential of the form

$$\Delta G_{\text{steric}}^{\text{in}} = \begin{cases} K_{\text{steric}} \cdot (z - z_{\text{in}})^2, & z \geq z_{\text{in}} \\ 0, & z < z_{\text{in}} \end{cases} \quad (8)$$

$$\Delta G_{\text{steric}}^{\text{out}} = \begin{cases} K_{\text{steric}} \cdot (z - z_{\text{out}})^2, & z \leq z_{\text{out}} \\ 0, & z > z_{\text{out}} \end{cases}$$

Our strategy for obtaining  $K_{\text{steric}}(z_i)$  and  $\zeta_o(z_i)$  is based on trying to choose those parameters that maximizes the similarity between the BD of the implicit model and the MD of the explicit model. In particular we optimize the parameters in Eq. 8 by requiring the BD model should give similar penetration time as the explicit MD simulation (the penetration time is evaluated by applying external forces that accelerate the penetration process and allow us to study it by direct MD). Our optimization process starts by choosing the “envelope” of the actual channel as a guide for the  $z$  dependence of  $\zeta_o$ , and then to fit the BD and MD of the neutral atoms ( $K^0$  and  $Na^0$ ) by adjusting  $K_{\text{steric}}$  and  $\zeta_o$ . More specifically, we first create the “imprint” of the inner part of the channel by generating a cubic grid (with 1 Å spacing), and then delete all grid points that are within 1.5

Å from any protein atom [the same approach is used in our Langevin dipole (LD) model<sup>26</sup>]. The outer envelope of the grid,  $\xi_0(z_i)$ , is described by its largest  $x$  and  $y$  values for each  $z$  ( $x(z_i)$  and  $y(z_i)$  respectively). In this way we can write:

$$\xi_0(z_i) = \xi_i(z_i) + \Delta_0 = \sqrt{x(z_i)^2 + y(z_i)^2} + \Delta_0 \quad (9)$$

where the  $x$  and  $y$  are the outer grid points for the specific  $z_i$ . Next we refine  $\Delta_0$  and  $K_{\text{steric}}$  by forcing the  $\langle z(t) \rangle$  obtained by BD simulation of the neutral atom, under an external force to reproduce the corresponding MD results. The corresponding fitting will be described in the next section. Note that a similar envelope can be generated by different methods (e.g., using the program HOLE<sup>32</sup>).

Another important aspect of our model is the selection of the optimal  $\gamma_z$  for Eq. (1). Here we note that the motion inside the channel corresponds to a motion under the influence of an effective potential rather than to a free diffusion. Thus the values of friction obtained by integrating of velocity autocorrelation function<sup>24</sup>:

$$\gamma = \left( \frac{3k_b T}{m} \right) \left( \int_0^\infty \langle \dot{r}(0) \dot{r}(t) \rangle dt \right)^{-1} \quad (10)$$

as was done in previous studies (e.g., Ref. 33), is not applicable to Eq. 1. More specifically, Eq. 10 gives  $\gamma$  for a free Brownian particle while Eq. (1) involves a gradient of an effective potential. With this problem in mind, we try to use a more realistic approximation of ion friction, namely we fit the velocity autocorrelation function  $C_v(t)$  and its power spectrum  $P_v(\omega)$  (obtained from MD simulations) to the analytical expression of Brownian (damped) harmonic oscillator (see Wang and Uhlenbeck<sup>34</sup>):

$$C_v(t) = \langle \dot{r}(0) \dot{r}(t) \rangle = \frac{k_b \cdot T}{m} \cdot \exp\left(-\frac{1}{2} \gamma \cdot t\right) \times \left[ \cos(\omega_1 \cdot t) - \frac{\gamma}{2 \cdot \omega_1} \cdot \sin(\omega_1 \cdot t) \right] \\ P_v(\omega) = \frac{\gamma \cdot k_b \cdot T \cdot \omega^2}{m \cdot [(\omega_0^2 - \omega^2)^2 + \gamma^2 \cdot \omega^2]}, \quad (11)$$

where  $\omega_0$  is angular frequency of undamped harmonic oscillator (eigenfrequency) and  $\omega_1 = \sqrt{(\omega_0^2 - (\gamma/2)^2)}$  is the shifted angular frequency (we assume the underdamped regime, when  $\omega_1$  is real). Since the ion spends most of the time near free energy minima, we can use the harmonic expansion of the free energy profile at the minima and then calculate the friction using the above formula.

The effect of an external field (the  $\Delta\Delta G_{\text{ext}}/\partial r_{i\alpha}$  term of eq. (1)) was not included in our previous studies, which corresponded to a zero external field. Now, however, we would like to examine the effect of the potential across the membrane. Here we use the simplest approach, writing

$$\partial\Delta G_{\text{ext}}/\partial z_i = F\Delta V/|z_{\text{in}} - z_{\text{out}}| \quad (12)$$

where  $\Delta V$  is the potential across the membrane and  $F$  is the Faraday constant. Obviously, one can use a more microscopic approach, placing actual charges on the two planes outside the simulation region to induce a field that will correspond to the macroscopic field. However, the approximation of Eq. (12), which has been used in the insightful studies of Chung et al.<sup>22</sup> seems to provide a reasonable way for estimating the effect of external potentials.

The van der Waals parameters used in the *microscopic* simulations are, of course, of major importance in simulations of ion selectivity. In this work, we optimized and/or varied these parameters by reproducing the selectivity in the binding of  $K^+$  and  $Na^+$  to valinomycin.<sup>35</sup> This was done for two sets of parameters, one set for the polarizable ENZY MIX force field<sup>36</sup> and the other for the non-polarizable ENZY MIX force field.<sup>36</sup> The parameters obtained for the 6–12 van der Waals potential of the polarizable force field were  $A = 150 \text{ kcal mol}^{-1} \text{ \AA}^{12}$ ,  $B = 4.35 \text{ kcal mol}^{-1} \text{ \AA}^6$  for  $K^+$  and  $A = 35.0 \text{ kcal mol}^{-1} \text{ \AA}^{12}$ ,  $B = 3.86 \text{ kcal mol}^{-1} \text{ \AA}^6$  for  $Na^+$  for the polarizable force field. Similarly, we obtained for the non-polarizable force field  $A = 522.7 \text{ kcal mol}^{-1} \text{ \AA}^{12}$ ,  $B = 4.35 \text{ kcal mol}^{-1} \text{ \AA}^6$  for  $K^+$ , and  $A = 143.7 \text{ kcal mol}^{-1} \text{ \AA}^{12}$ ,  $B = 3.89 \text{ kcal mol}^{-1} \text{ \AA}^6$  for  $Na^+$ . The later set is identical to the set refined by Aqvist<sup>37</sup> by considering the solvation energy of  $K^+$  and  $Na^+$  in water.

It might be useful to point out that we view our parameterization to be valid despite the fact that the absolute solvation energies are evaluated relative to the hydration energy of a proton, whose estimate has changed somewhat in recent years.<sup>38</sup> However, all of our studies involve the deference between the solvation of ions ( $K^+$  and  $Na^+$ ) rather than the absolute values. Furthermore, the penetration profile involves movement of the ion from water (not from vacuum) to the protein. Here the most crucial point is the requirement that the parameterization will reproduce the difference between the protein-ion and protein-water interaction and this was verified in part in our valinomycine study.<sup>35</sup>

The microscopic simulations (for both the LRA and the FEP calculations) were done by using the same surface constraint all atom solvent (SCAAS) boundary conditions<sup>39</sup> and local reaction field (LRF) model<sup>40</sup> used in Burykin et al.<sup>20</sup> as implemented in the ENZY MIX module of the MOLARIS programs.<sup>36</sup> The membrane region was represented by a grid of induced dipoles as described in Burykin et al.<sup>20</sup> The semimacroscopic PDL D/S-LRA calculations were done with the POLARIS model of the program MOLARIS. The details of this approach are provided elsewhere (e.g.,<sup>36</sup>) and also in Burykin et al.<sup>20</sup>

With the single ion profiles, generated by the PDL D/S-LRA calculations and the ion-ion potential of Eq. (4), we moved to the actual simulation of the ion current in the system described in Figure 1. The simulations were performed by solving numerically the Langevin equation [Eq. (1)] for a simulation system with the specific free energy profile and with 4  $K^+$  and 4  $Cl^-$  ions in both the extracellular and intracellular sides (this corresponds to a concentra-

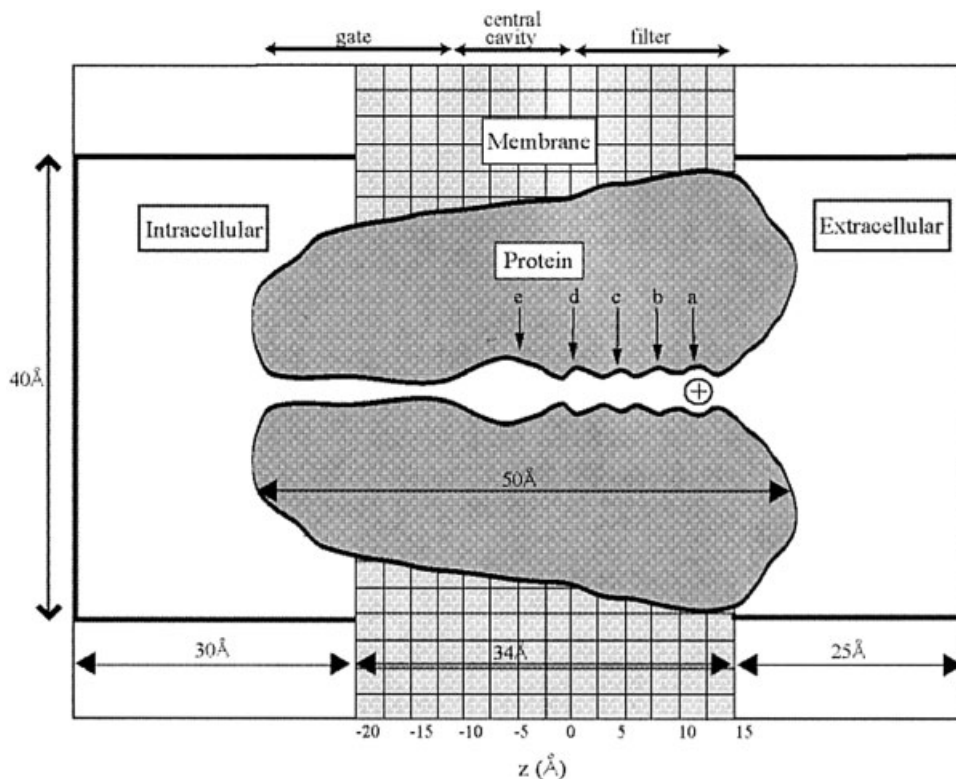


Fig. 1. Schematic description of the system used in the BD simulations. The wide black lines designate the actual boundaries of the simulation system.

tion of 200 mM in both sides) and an external potential of 200 mV. This was done using the program CHANNELIX.<sup>20</sup>

### MAPPING MICROSCOPIC ENERGY AND DYNAMICS ON A SIMPLIFIED MODEL

#### Free Energy Profiles

The first step in our approach involved the evaluation of the effective free energy surface  $\Delta G(r)$ . We started by calculating the potential for a single  $K^+$  ion and a single  $Na^+$  ion by the PDL/D/S-LRA method. The profile for  $K^+$  was already evaluated in our previous study.<sup>20</sup> However, this time we used a better calibrated set of parameters (see Simulation Methods) to generate the protein configurations for the PDL/D/S semimacroscopic calculations. The calculations were done by moving gradually from  $z = -35$  Å to  $z = 25$  Å in 0.3-Å increments. In each point, we constrained the ion by a harmonic constraint of  $300 \text{ kcal} \cdot \text{mol}^{-1} \cdot \text{Å}^{-2}$  and performed 30 of PDL/D/S-LRA calculations each with 15 ps MD on the charged and uncharged form of the given ion. The average of the ion-environment interaction of these calculations (see Burykin et al.<sup>20</sup>) gave the  $\Delta \Delta G_{\text{self}}$  for the given position  $z$ .

The calculated free energy profiles (Fig. 2) were obtained by averaging the PDL/D/S-LRA results, obtained with the two parameters sets (for polarizable and nonpolarizable force fields). This is a reasonable way to reduce the error range of the calculations since both approaches are equally valid, as much as the generation of structures for the

PDL/D/S model are concerned. Also note that the minima of the  $K^+$  profile do not coincide exactly with the positions of the loading states (which are given in Fig. 1). This might reflect the fact that we are dealing with a single ion profile while the structural studies correspond to occupation by two ions or more (see below). At any rate, as seen from Figure 2, the maxima of the profiles for  $K^+$  and  $Na^+$  do not overlap each other (see also below) and the activation barriers (relative to bulk water) for  $Na^+$  are 2–3 kcal/mol higher than the corresponding barriers for  $K^+$ . These results may be compared to the 5.4 kcal/mol obtained by the FEP calculations of Allen et al.<sup>9</sup> and the about 2.1 kcal/mol free energy difference obtained at the minima of the second loading state by the FEP calculations of Luzhkov and Åqvist<sup>8</sup> (see also below).

It might be useful to comment at this point on the nature of the single ion calculations and on the crucial point that these calculations (with a single ion) are used to generate the effective potential for multi-ion trajectories. Luzhkov and Åqvist<sup>8</sup> found that the channel is not stable in a single ion simulation. This seems to be consistent with experimental findings. On the other hand, our 50-ps relaxation run with a single ion in its charged and uncharged forms did not involve major collapses. It should be noted that our studies were done with a 22 Å SCAAS simulation sphere with a fixed membrane region and a fixed protein outside the simulation region. Also it should be noted that the protein did collapse in single-ion simulations that did not

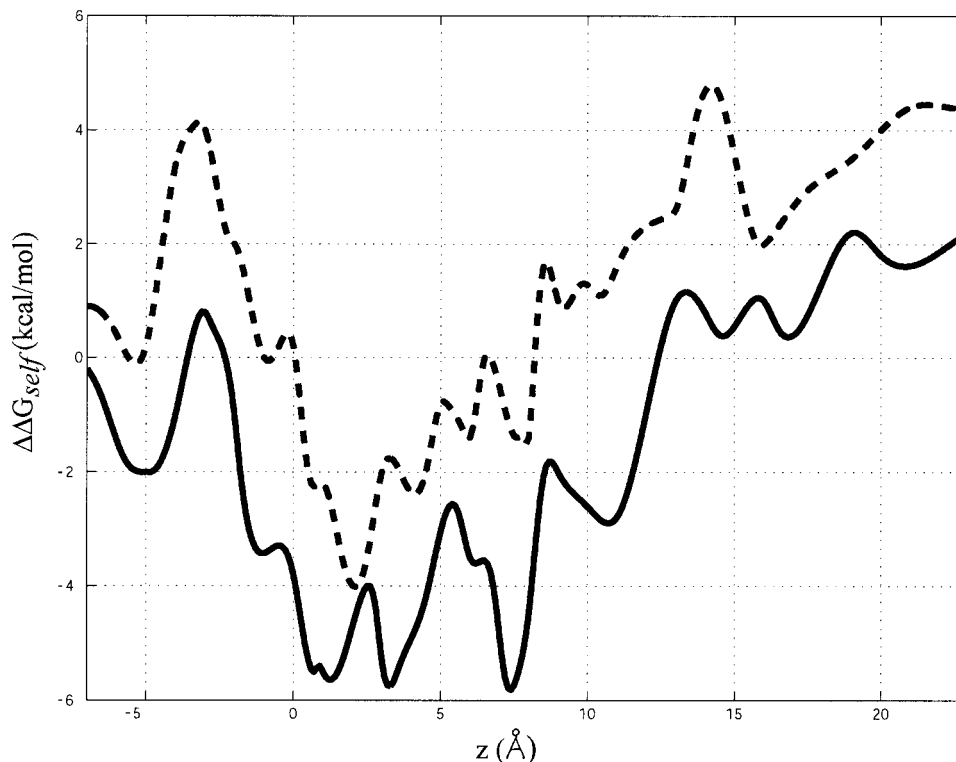


Fig. 2. The PDL/S-LRA profile for  $K^+$  (—) and  $Na^+$  (---) single ion transfer through the KcsA selectivity filter.

include the SCAAS constraint. Now, the key point is that we do not try to reproduce or to study possible slow unfolding processes but to explore the ion current in the conducting form of the channel. Here the relevant model for ion current calculation should not allow for a channel collapse, since the single ion profile is used for calculations of the potential of multi-ion trajectories and even when the trajectory involves a single ion (rather than several ions) it involves a time that is not sufficient for unfolding.

The treatment of the gate region ( $-30 \text{ \AA} < z < -10 \text{ \AA}$ ) is similar to the approach used in our previous study.<sup>20</sup> As discussed and demonstrated in Burykin et al.,<sup>20</sup> the X-ray structure corresponds most probably to the closed state of the gate. Fortunately, there is evidence that the structure of the filter region does not change in a drastic way during the transition from the open to closed state.<sup>41</sup> Furthermore, the reorganization of the filter region during an LRA charging process is probably similar in the open and closed forms. Thus, we consider the X-ray structure of the filter region as a good starting point for studies of this region and also assume that the barriers in the gate region in its open state are smaller than the barriers in the filter region. With this in mind, we used a barrierless solvation potential for the gate region, while simulating the current for the open state. This working hypothesis is identical to the implicit assumption of most previous simulation studies (e.g., Refs. 16,19) where the gate region is not considered at all. Furthermore, this is probably the most logical working hypothesis before one has clear structural information on the open state of the gate region. The possible effect

of the gate region on the selectivity is discussed in Concluding Remarks.

Although our actual modeling involves only a single ion profile and the interaction between the ions is treated by the effective potential of Eq. 4, it is useful to explore some selective sections along the free energy surface of a two-ion system. The most instructive sections is the profile for a transfer of two ions with a separation of  $7 \text{ \AA}$  (this corresponds to a concerted transfer were the ions occupy the  $n$  and  $n+2$  loading sites). This type of profile has been evaluated by the PDL/S-LRA method and is given in Figure 3. As seen from the figure, the profile for  $2Na^+$  ions is shifted to higher energy than the profile of  $2K^+$  (note that the actual simulations did not fix the ions at  $7 \text{ \AA}$  separation). The significance of this observation will be discussed below.

As an alternative estimate of the free energy profiles, we also tried to evaluate the free energy of mutating  $K^+$  to  $Na^+$ , as well as for a sequential cycle that gives the free energy for mutating two  $K^+$  ions to two  $Na^+$  where the two ions are separated by  $\sim 7 \text{ \AA}$ . This was done with different sets of position constraints. The calculation at each point involved a FEP simulation with 30 windows and 50 ps for each window. The calculations with relatively weak constraints gave the results summarized in Table I (note that the results reported in Table I were obtained in a very different way than the results presented in Figs. 1 and 2). The calculated FEP results that correspond to the minima of the loading states are similar in many respects to the corresponding results of Luzhkov and Aqvist,<sup>8</sup> considering

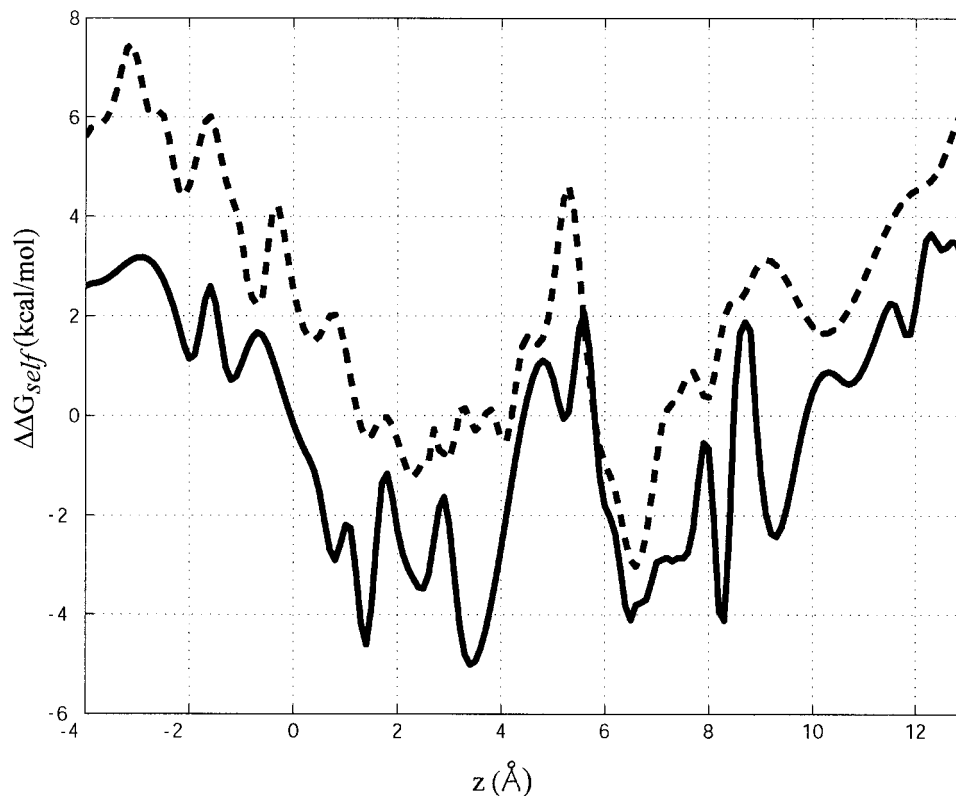


Fig. 3. The PDL/S-LRA profile for the transfer of two  $K^+$  (—) and two  $Na^+$  (---) ions through the KcsA selectivity filter. The calculations were done with the second ion kept at 7 Å from the first ion (the  $z$  coordinate corresponds to the coordinate of the first ion and the coordinate of the second ion is taken as  $z+7$ Å.). Note that this profile is only one possible section in the two-ion free energy surface and that we are not using it in our calculations (the actual simulations used Eq. 4 and did not fix the ion-ion distance).

**TABLE I. FEP Calculations of Mutations of  $K^+$  to  $Na^+$  in Different Sites of the KcsA Channel<sup>†</sup>**

Mutation	Occupation	$\Delta G_p(nK^+ \rightarrow nNa^+)$	$\Delta G_w(nK^+ \rightarrow nNa^+)$	$\Delta\Delta G(nK^+ \rightarrow nNa^+)$
$K^+ \rightarrow Na^+$	(1)0000	-15.92	(-17.58)	1.66
	0(1)000	-19.70		-2.12
	00(1)00	-15.98		1.60
	000(1)0	-17.87		-0.29
$2K^+ \rightarrow 2Na^+$	(1)0(1)00	-29.53	(-35.16)	5.63
	0(1)0(1)0	-31.44		3.72
$K^+ \rightarrow Na^+$	(1)0001	-16.20	(-17.58)	1.38
	0(1)001	-16.05		1.53
	00(1)01	-13.65		3.93
	000(1)1	-18.07		-0.49
$2K^+ \rightarrow 2Na^+$	(1)0(1)01	-32.21	(-35.16)	2.95
	0(1)0(1)1	-31.20		3.96

<sup>†</sup>All energies are in kcal/mol. The notation for the occupation of the loading states is based on the order a, b, c, d, e, where 1 and 0 correspond to an occupation by an ion and by a water molecule, respectively. The ions that were included in region I are given in parentheses. The notations p and w correspond to protein and water, respectively. The reported results represent an average of 3 simulations (each of 30 windows and 3.0 ps in each window) using different initial conditions. The calculation involved  $3.0 \text{ kcal} \cdot \text{mol}^{-1} \text{ \AA}^{-2}$  position constraints on the positions of the indicated ions. The free energies of the mutations in water are given in brackets.

the fact that the calculations of Luzhkov and Aqvist<sup>8</sup> were done with an extra ion in the central cavity. The calculations with a  $20 \text{ kcal mol}^{-1} \text{ \AA}^{-2}$  constraint gave unstable results, where the mutation free energy was positive at the loading state and negative at the halfway between these

states. It appears that at least a part of the problem is due to the fact that the profiles of the  $K^+$  and  $Na^+$  ions do not have maxima at the same points. Apparently, our FEP calculations cannot give a sufficiently reliable mutation profile in the selectivity filter, although the results at the

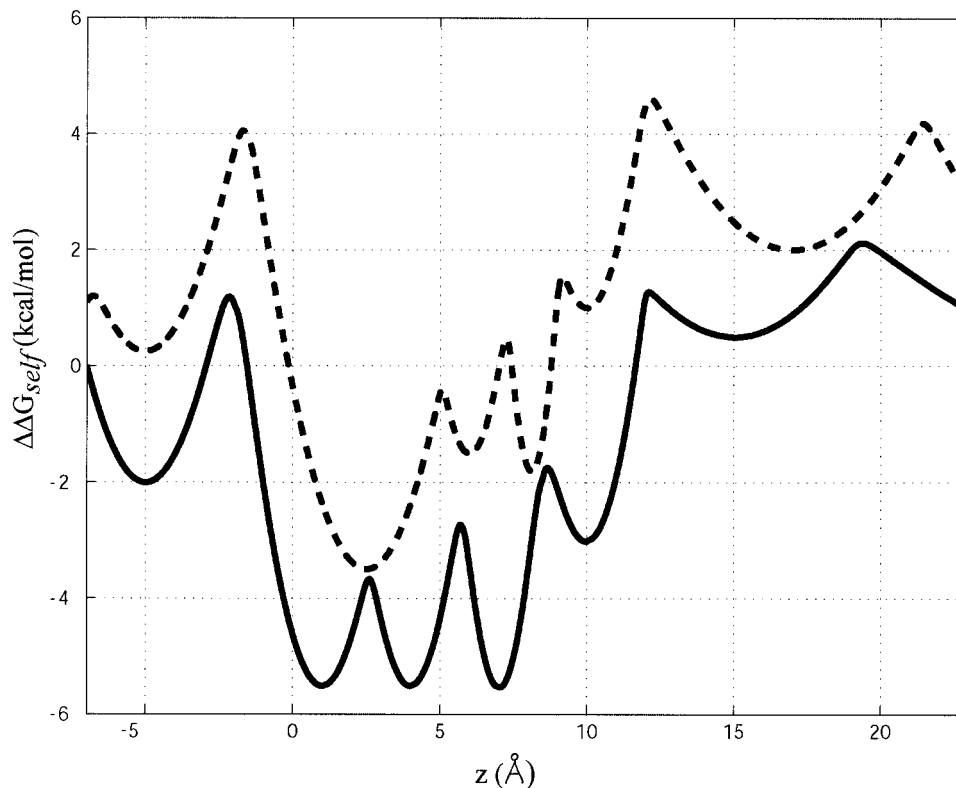


Fig. 4. The analytical single ion profile for  $K^+$  (—) and  $Na^+$  (---) ions. These potentials were obtained by Eq. 13 and fitted to the corresponding profiles in Figure 1.

minima with a weak constraint (that allows the ions to sample all the minima region) are reasonable. Our attempt to evaluate all-atom PMF were also discouraging, providing very large hysteresis and reflecting convergence difficulties in the filter region (see also Edwards et al.<sup>31</sup>). It seems to us that current PMF calculations are sufficiently reliable to provide quantitative results for transfer of ions from water to the KcsA interior (see also discussion in Burykin et al.<sup>20</sup>), although such calculations might be effective for studies of motion of the ions between neighboring sites.

In view of the difficulties in obtaining a stable profile from the formally rigorous approaches, we prefer to rely on the more stable semimacroscopic results, while keeping in mind the mutations results from the all-atom microscopic modeling at the minima of the loading states. Thus, we will focus our discussion on the PDL/S-LRA results of Figure 2.

In order to facilitate further analysis, we also converted the key features of the potential of Figure 2 to a simplified analytical potential whose parameters can be changed in a systematic way. That is, we represented the single ion profile by an empirical valence bond (EVB)-type potential,<sup>26</sup> where we considered  $n$ -interacting parabolic potentials and look for the lowest eigenvalue of the Hamiltonian.

$$\begin{aligned} H_{ii} &= K_i(z_i - z_o^i)^2 + B_i \\ H_{ij} &= \Delta_{ij} \end{aligned} \quad (13)$$

where  $z_o^i$  and  $K_i$  are the minimum and force constant of the  $i$ th state. The mixing term  $\Delta_{ij}$  is taken as zero for non-overlapping parabolas. The use of the EVB surface is similar to the approach used in our studies of proton translocation in proteins,<sup>23</sup> although in the case of ion channels the method simply provides a fitting tool rather than as a way of capturing the physics of bond breaking, bond making processes. The resulting simplified analytical potentials are given in Figure 4.

As seems obvious from Figures 2 and 4 and from other related calculations (e.g., Ref. 9) the penetration profile of the  $Na^+$  ion is shifted up relative to the profile of the  $K^+$  ion. It is also obvious that at least at some points the profiles do not overlap each other (see below). It is not clear, however, how much the up-shift of the single  $Na^+$  profile contributes to the selectivity. Another interesting feature, and in some respects an open question, is the nature of the profile for concerted two ions motion at 7 Å separation (again note that we do not use this potential in our BD simulations). As indicated by the calculations of Luzhkov and Åqvist<sup>8</sup> and by the some of our microscopic simulation, the free energy change upon mutating  $2K^+$  ions to  $2Na^+$  ions ( $\Delta\Delta G(2K^+ \rightarrow 2Na^+)$ ) at the minima of the loading states is significantly larger than the free energy of mutating a single ion ( $\Delta\Delta G(K^+ \rightarrow Na^+)$ ). If these results were also valid for the maxima of the corresponding energy profile, we could assume that the ion-ion interaction is larger for  $Na^+ - Na^+$  than for  $K^+ - K^+$  at any point in the

**TABLE II. Some Parameters Used for the Effective Potential in BD Simulation<sup>†</sup>**

Type of interaction	Function	Equation	Parameters	Values
Ion-ion:electrostatic	$\epsilon_{\text{eff}}(r) = 1 + \epsilon'(1 - \exp(-ar))$	(5)	$\epsilon'$ $a$	30.0–15.0 $0.1 \text{ \AA}^{-1}$
Ion-ion:steric	$\Delta G'(r_{ij}) = Ar^{-8} + K_{\text{filter}}(z_{ij} - z_{ij}^0)^2$	(6)	$A$ $K_{\text{filter}}$ $z_{ij}^0$	1.5 A 1.0 kcal mol <sup>-1</sup> Å <sup>-2</sup> 7.0 A
Ion-channel:steric	$\Delta G_{\text{steric}}^{\text{channel}}(x_i, y_i, z_i) = \begin{cases} K_{\text{steric}} \cdot (\xi_i - \xi_0(z_i))^2, & \xi_i \geq \xi_0(z_i) \\ 0, & \xi_i < \xi_0(z_i) \end{cases}$	(7)	$K_{\text{steric}}$ $z_{\text{in}}$ $z_{\text{out}}$	5.0 kcal mol <sup>-1</sup> Å <sup>-2</sup> –30.0 Å 20.0 Å
	$\Delta G_{\text{steric}}^{\text{in}} = \begin{cases} K_{\text{steric}} \cdot (z - z_{\text{in}})^2, & z \geq z_{\text{in}} \\ 0, & z < z_{\text{in}} \end{cases}$	(8)	$\Delta_0$	1.0 Å for K <sup>+</sup> ; 0.9 Å for Na <sup>+</sup>
	$\Delta G_{\text{steric}}^{\text{out}} = \begin{cases} K_{\text{steric}} \cdot (z - z_{\text{out}})^2, & z \geq z_{\text{out}} \\ 0, & z < z_{\text{out}} \end{cases}$			(see comment <sup>†</sup> )
	$\xi_0(z_i) = \xi_i(z_i) + \Delta_0 = \sqrt{x(z_i)^2 + y(z_i)^2} + \Delta_0$	(9)		

<sup>†</sup>The actual simulations were accelerated by using  $\Delta_0 = 2.5 \text{ \AA}$  for both K<sup>+</sup> and Na<sup>+</sup> ions and then scaled down by a factor of four (for discussion, see Mapping the Friction and Steric Effects).

selectivity filter. However, the results obtained from the FEP calculations at the maxima of the profile are very unstable, and the PDL/D/S-LRA method accounts for almost all the increase in  $\Delta\Delta G(2\text{K}^+ \rightarrow 2\text{Na}^+)$ , relative to  $\Delta G(\text{K}^+ \rightarrow \text{Na}^+)$ , by the corresponding single ion contribution (rather than the ion-ion interaction). Furthermore, the PDL/D/S-LRA calculations do not provide an indication of the increase of the ion-ion interaction for  $2\text{Na}^+$  at the maxima of the corresponding free energy profiles. At any rate, we are going to explore below the possible implications of this interesting effect.

### Mapping the Friction and Steric Effects

As stated in Simulation Methods, we evaluated the friction coefficients by fitting the analytical expression of the velocity autocorrelation of Brownian harmonic oscillator (Eq. 11) to the velocity autocorrelation obtained from microscopic MD simulation of the motion in the  $z$  direction at the loading sites. Since the friction coefficients are strongly correlated with the harmonic frequency,  $\omega$ , we took  $\omega$  from the power spectrum of the velocity autocorrelation. The resulted fitting gave  $\gamma_{z, \text{K}^+} = 10 \text{ ps}^{-1}$ ,  $\gamma_{z, \text{Na}^+} = 15 - 25 \text{ ps}^{-1}$ . These values are somewhat tentative since it is impossible to obtain a perfect fitting between Eq. (11) and the microscopic  $C(t)$  without using effective frequencies that do not correspond to the free energy profile. Obviously, determining what is the best phenomenological way to describe the microscopic autocorrelation is an interesting topic,<sup>42</sup> but we do not view it as the central issue in our selectivity studies. In fact, we believe that the best option to determine the optimal  $\gamma_z$  is to perform MD simulations with an external force and then to force (by adjusting  $\gamma_z$ ) the corresponding BD simulations to reproduce the same average motion in the  $z$  direction. This approach is left, however, to subsequent studies. At any rate, our starting values for  $\gamma$  are  $\gamma = \gamma_z = 10 \text{ ps}^{-1}$  for K<sup>+</sup> inside the channel  $\gamma = \gamma_z = 25$  for Na<sup>+</sup> inside the channel and then  $\gamma_{\text{K}^+} = 33 \text{ ps}^{-1}$ ,  $\gamma_{\text{Na}^+} = 81 \text{ ps}^{-1}$  in water, (the

values in water were taken as the corresponding experimental values).

In order to determine the effective steric parameter for the motion in the  $x, y$  direction, we follow the idea outlined in Simulation Methods. That is, after determining  $\zeta_i(z_i)$  (see Simulation Methods), we started by running a series of microscopic MD simulation of the uncharged K<sup>0</sup> and Na<sup>0</sup> atoms taking  $z = 20 \text{ \AA}$  (with different values of  $x$  and  $y$ ) as starting points and applying a force of  $F \sim 4 \text{ kcal mol}^{-1} \text{ \AA}^{-1}$  toward the channel interior. The same force was then applied in the BD simulations with different values of the  $K_{\text{steric}}$  and  $\Delta_0(z)$  of Eq. 7. The best agreement between the BD and MD permeation times were obtained with  $K_{\text{steric}} = 5 \text{ kcal mol}^{-1} \text{ \AA}^{-2}$  and  $\Delta_0 = 1.0$  and  $0.9 \text{ \AA}$  for K<sup>0</sup> and Na<sup>0</sup>, respectively, for the selectivity filter region. We also found that the current is proportional to the square of the channel radius ( $\Delta_0 + \zeta(z_i)$ ). With this in mind and in order to obtain accelerated convergence, we used  $\Delta_0 = 2.5 \text{ \AA}$  for both K<sup>0</sup> and Na<sup>0</sup>. Thus, with  $\zeta(z_i) = 0.5 \text{ \AA}$  at the narrow points of the channel we have to scale down our calculated current by a factor of four.

The parameters obtained from the above considerations as well as other parameters of the effective potential are summarized in Table II. We would like to clarify in this respect that this are not free parameters that were chosen to reproduce to the observed selectivity but parameters that are obtained from microscopic considerations (see also discussion in Concluding Remarks).

### EXAMINING THE ORIGIN OF THE SELECTIVITY OF THE KCSA ION CHANNEL

Although the free energy profiles obtained in the previous section may give strong hints for the origin of the selectivity, they cannot provide a conclusive answer (even if the results were fully quantitative). That is, the K<sup>+</sup>/Na<sup>+</sup> selectivity expresses the difference between the corresponding ion currents. Thus, it is essential to convert the free energy profiles and friction coefficients to the correspond-

**TABLE III. Simulated Currents for K<sup>+</sup> and Na<sup>+</sup> in Different Conditions<sup>†</sup>**

Case	Ion	$\gamma$ , ps	$\epsilon'$	Concentration: in/out, mM	$\Delta V$ , mV	Solvation profile <sup>a</sup>	I, pA	Selectivity
A	K <sup>+</sup>	10	30	200/200	200	Numerical	10.00	—
B	Na <sup>+</sup>	25	30	200/200	200	Numerical	0.25	40
C	K <sup>+</sup>	10	30	200/200	200	Analytical	5.00	—
D	Na <sup>+</sup>	25	30	200/200	200	Analytical	0.25	20
E	Na <sup>+</sup>	25	30	200/200	200	Analytical, +2.0 kcal/mol at the a-out barrier	0.025	200
F	Na <sup>+</sup>	25	30	200/200	200	Analytical, +2.0 kcal/mol at the e-d barrier	0.02	250
G	Na <sup>+</sup>	25	30	200/200	200	Analytical, -1.0 kcal/mol at the minima	0.01	500
H	K <sup>+</sup>	10	30	200/200	200	Analytical (equal depth at the minima) <sup>b</sup>	6.75	—
I	Na <sup>+</sup>	25	30	200/200	200	Analytical (equal depth at the minima) <sup>b</sup>	0.15	45
J	K <sup>+</sup>	10	30	200/200	400	Analytical	17.50	—
K	Na <sup>+</sup>	25	30	200/200	400	Analytical	1.75	10
L	Na <sup>+</sup>	10	30	200/200	200	Analytical	0.75	7
M	K <sup>+</sup>	25	15	200/200	200	Analytical	8.00	—
N	K <sup>+</sup>	10	30	400/200	200	Analytical	10.00	—
O	Na <sup>+</sup>	25	30	400/200	200	Analytical	0.36	27
P	K <sup>+</sup>	10	30	400/200	400	Analytical	29.00	—
Q	Na <sup>+</sup>	25	30	400/200	400	Analytical	2.25	13

<sup>†</sup>All quantities are in the indicated units.  $\gamma$ ,  $\epsilon'$ , and  $\Delta V$  designate, respectively, the friction in Eq. (1), the scaling parameter in the effective dielectric of Eq. (5), and the external potential. The calculated current is divided by four to account for the use of larger channel radius (see Mapping the Friction and Steric Effects).

<sup>a</sup>The solvation profiles used are either the numerical PDL/D/S-LRA potentials (A and B) or the indicated modifications of the analytical potentials.

<sup>b</sup>The analytical potentials were modified in a way that the total potential (solvation potential + interaction with the ionized groups + external potential) will have minima of equal depth. The selectivity is obtained as the ratio between the currents of K<sup>+</sup> and Na<sup>+</sup>. Thus we give the relevant selectivity in the corresponding entry for Na<sup>+</sup>.

ing currents, in order to see if a given model can account for the observed selectivity.

Our ability to calculate ion currents helps not only in evaluating the selectivity that corresponds to the calculated free energy profile, but also in examining what can account for the selectivity within the error range of the free energy calculations. Furthermore, the calculations can help in examining what is the role of the different features of the free energy profile in controlling the ion current. Of course, this can be easily done with more phenomenological approaches (e.g., Ref. 5), but with such models we face the risk of going out of the range of physically feasible parameters (see Concluding Remarks).

Our current calculations started with the PDL/D/S-LRA profile for the single-ion motion and with  $\epsilon' = 30$  for both the Na<sup>+</sup> and K<sup>+</sup> ions (sets A and B). The calculations involved external potential of 200 mV and equal concentrations (C = 200 mM) on both sides of the membrane, (this corresponds to the experimental conditions in LeMasurier et al.<sup>6</sup> where the observed K<sup>+</sup> current is 15 pA). The calculated currents are given in Table III. Similar currents and selectivity were obtained from the analytical EVB-like potential (Fig. 3) that was fitted to the PDL/D/S-LRA potential (sets C and D). As seen from Table III, we obtained selectivities of 40 and 20 for the numerical and analytical potentials, respectively. This selectivity is quite significant but still underestimates the observed selectivity (although the calculated selectivity is expected to

increase at lower external potential). With this in mind, we used our analytical model to examine different factors that can account for the observed selectivity. The idea is to try to modify the analytical potential as little as possible while trying to obtain a reasonable selectivity. The simplest way to reproduce the selectivity is to increase the highest barriers in the single ion profile. Increasing the exit (a-out) barrier by 2.0 kcal/mol (set E) or increasing the entry (e-d) barrier by 2.0 kcal/mol (set F) increases the selectivity to 200 and 250, respectively. Another effective way to increase the selectivity is to push down the minima of the Na<sup>+</sup> profile (set G).

Additional interesting effects that can be observed from Table III include the relatively small dependence on friction (approximately linear dependence) and the dependence on the external potential.

Typical simulated trajectories and currents for K<sup>+</sup> and Na<sup>+</sup> are shown in Figure 5. As seen from Figure 5, the Na<sup>+</sup> ion needs much longer time than the K<sup>+</sup> ion to pass through the channel. The ability to simulate these longer times, which is crucial for our studies, is obviously not provided at present by direct MD simulation (see Shrivastava et al.<sup>10</sup>).

As seen from Figures 5 and 6, K<sup>+</sup>, the productive trajectories (trajectories that leads to ion transport) tend to be more concerted (the ions tend to move together through the filter), while the Na<sup>+</sup> productive trajectories tend to involve a single ion transport through the selectiv-

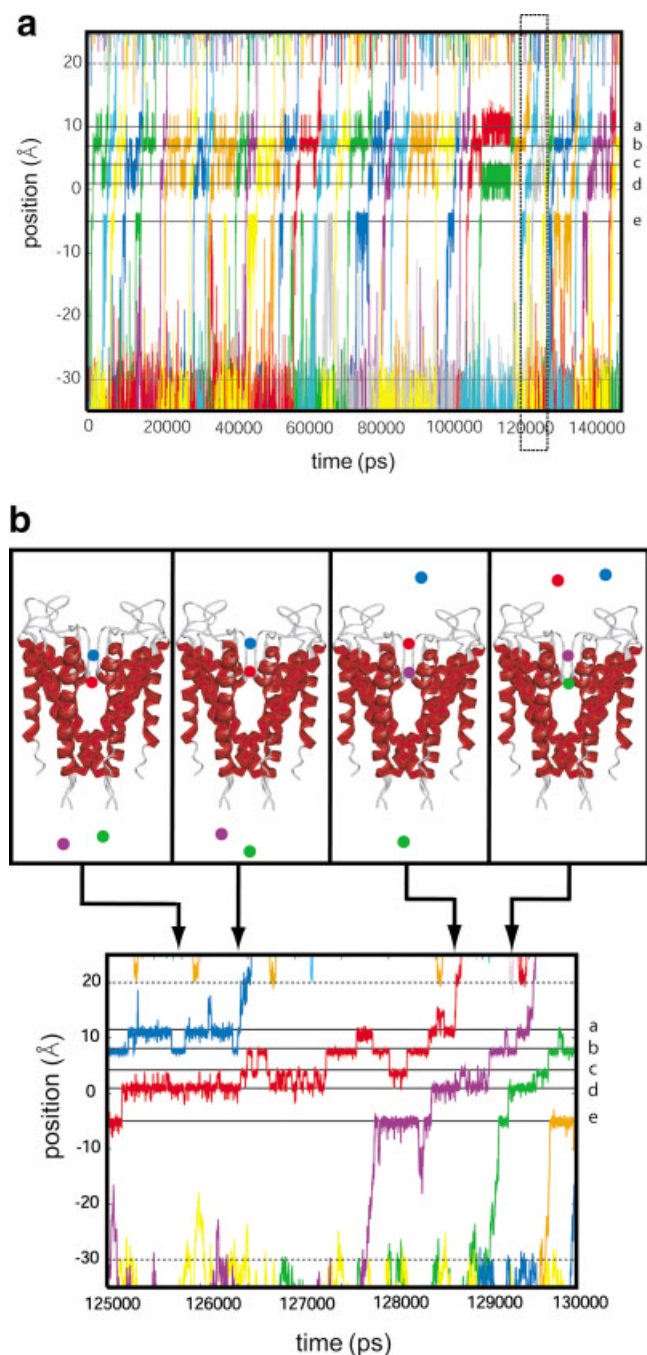


Fig. 5. Trajectories of K<sup>+</sup> ions in the KcsA channel. (a) A long trajectory ( $z$  as a function of time) that was used in calculating the ion current. (b) A segment from the long trajectory taken from the dashed rectangle of (a). The positions of the ions during the trajectory are described by snapshots that depict only those ions which reside in the channel at some period during the time shown.

ity filter. However, the degree of concertedness appears to depend on the concentration and the applied potential. That is increasing the external potential and the concentration gradient tends to lead to more concerted trajectories. Furthermore, assuming a more regular spacing for the minima of the Na<sup>+</sup> profile leads to a partially concerted trajectory for this ion. Apparently the deeper are the

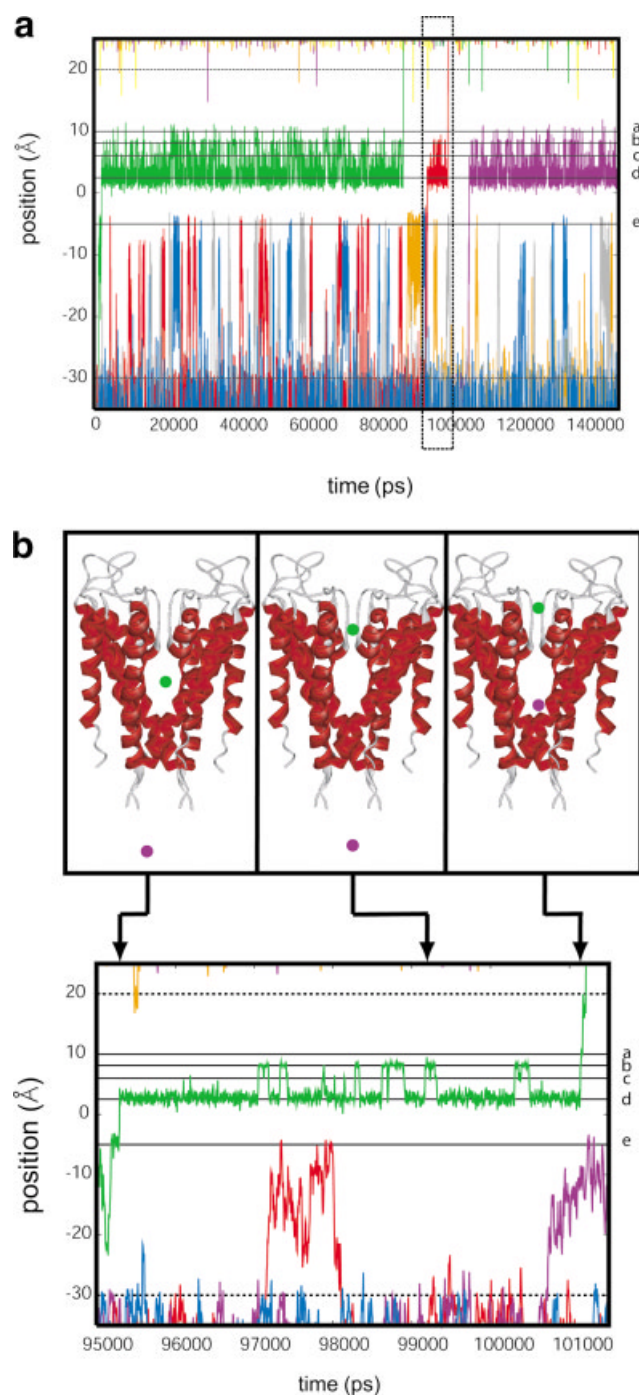


Fig. 6. Trajectories of Na<sup>+</sup> ions in the KcsA channel. (a) A long trajectory ( $z$  as a function of time) that was used in calculating the ion current. (b) A segment from the long trajectory taken from the dashed rectangle of (a). The positions of the ions during the trajectory are described by snapshots that depict only those ions which reside in the channel at some period during the time shown.

minima of the potential, the more the ions tend to be bound and to move in a concerted way.

An intriguing option is presented by the idea that the difference in ion-ion interaction contributes in a major way to the observed selectivity.<sup>8</sup> Although this idea was not

reproduced by PDL/D/S free energy profile, we decided to examine it by changing the effective dielectric for the ion-ion interaction. Since our  $\text{Na}^+$  trajectories did not follow concerted paths with our calculated free energy profiles and simulation conditions, we decided to use the concerted  $\text{K}^+$  trajectories as a test case for the situation expected in the case where the  $\text{Na}^+$  trajectories are concerted. Thus we decreased  $\epsilon'$  for the  $\text{K}^+ \cdots \text{K}^+$  interaction from 30 to 15 [this corresponds to a change of the corresponding ion-ion interaction from 2.9 to 5.5 kcal/mol (see Eq. 4) for 7 Å separation] and examined the corresponding changes in the behavior of the system. Surprisingly, the change in ion-ion interaction had only a small effect on the selectivity (compare sets C and M). Apparently the inability to obtain larger selectivity is due to the fact that when the ion-ion interaction increases, the current tends to include more contributions from single ion trajectories.

Another factor that did not appear to be so effective in controlling the selectivity is the relative height of the minima at the loading states. Changing the potential to give equal height at these minima (sets H and I) had only a small effect on the current of each ion. The sensitivity to the parameters in Table II was found to be relatively small in the region studied. The sensitivity to the  $\epsilon'$  has been considered above. The parameter A only affected the interaction with counterions and thus has no applicable effect. The parameters  $K_{\text{filter}}$  and  $z^0$  did not lead to a significant change in selectivity. Similarly,  $\Delta_0$  and  $K_{\text{steric}}$  have a small effect on the calculated selectivity.

### CONCLUDING REMARKS

In order to evaluate ion currents in ion channels in a reasonable computer time, it is essential to have effective potentials that can be evaluated in a fast and efficient way. Thus, it is tempting to combine semimacroscopic calculations with BD simulations. However, in doing so one faces major problems. First, the evaluation of the ion-ion interaction term by Poisson-Boltzmann (PB) and related approaches is at present too expensive (see discussion in Burykin et al.<sup>20</sup>), although this problem can be overcome by adopting our effective ion-ion potential [Eq. (5)]. Second, and more importantly from the point of view of the present work, most current macroscopic and semimacroscopic approaches are not expected to reproduce ion selectivity since they do not reflect in a consistent way the change in the channel radius upon exchange of  $\text{K}^+$  by  $\text{Na}^+$  (they only reflect this effect for the ions in water). More specifically, PB calculations do not consider the changes in the geometry of the channel loading sites upon the binding of different ions. Consequently, they would predict the same energy for  $\text{K}^+$  and  $\text{Na}^+$  inside the channel and lead to incorrect selectivity. Attempts to use MD-generated structures may help but will still miss the channel reorganization energy. Thus, one of the main advances of the present work is its ability to represent ion selectivity in a consistent way by a semimacroscopic method. This is due to the LRA formulation of our PDL/D/S-LRA approach, which takes into account in a consistent way the effect of the steric interaction between the ion and the channel and the corresponding reorganization energy.

The ability to obtain the proper trend in ion selectivity by our semimacroscopic calculations is encouraging progress.

Our computational approach allowed us to explore detailed features, which are hard to examine by more phenomenological approaches. For example, it is found that the degree of concertedness in the productive trajectories depends on the concentration and applied voltage. In our experience, it is hard to reproduce this result by a one-dimensional BD model with the same effective potential or by a master equation treatment. Although this issue will require further studies, we are quite certain that in some limiting cases the ion motion through the selectivity filter is less concerted than generally assumed. Most current suggestions for the origin of the selectivity of the KcsA channel do not involve any calculations of the corresponding multisite kinetics. One interesting exception is the proposal that involves explicit kinetic calculations was put forward by Morals-Cabral et al.<sup>5</sup>. This proposal assumed a reasonable kinetic mechanism and used the corresponding master equation to account for the difference in conduction of  $\text{K}^+$  and  $\text{Rb}^+$ . The main idea that emerges from this proposal is that in an optimal concerted ion movement, the free energy change  $\Delta G_0$  is zero, while in a non-optimal transport  $\Delta G_0 \neq 0$ . The present simulations indicate that the situation may be more complicated. More specifically, in our opinion it is extremely hard to construct a unique kinetic scheme based only on experimental and structural information. Thus, for example, the scheme of Morals-Cabral et al.<sup>5</sup> involves a step where two  $\text{K}^+$  move to a closer distance (steps F  $\rightarrow$  B) so that the energy of the system is expected to increase due to ion-ion interaction. However, according to the kinetic scheme of Morals-Cabral et al.<sup>5</sup>, the actual energy of the system decreases by 0.8 kcal/mol. While this situation is possible (with proper changes in the binding energy), it is not consistent with our free energy calculations, where the energy increases when two positive ions move to a closer distance in the selectivity filter. Thus, we believe that at present the optimal approach should involve a combination of structure-based energy calculation and experimental information.

One of the key points in our modeling approach is the attempt to insist (as much as possible) on a realistic and physically consistent treatment of the channel. In our view, and as argued in our previous study,<sup>20</sup> other reported macroscopic and semimacroscopic models have not used a sufficiently realistic treatment. One of the main problems is the selection of proper dielectric constants. Here it is not sufficient to argue that a model with some assumed protein dielectric constant reproduce the observed current, since this can be done with different models (which might be unable to account for the selectivity). It is essential to have a model that reproduces observed facts about binding, mutations, and  $\text{pK}_a$ s. Such validation studies have not been reported in the KcsA case but have been done by us and others for a long time on other proteins (e.g.,<sup>27</sup>). Our studies demonstrated that one cannot use a low  $\epsilon_p$  for charge-charge interactions and that models that do not involve the LRA treatment must use

$\epsilon_p > 6$  to correctly account for the self energy of the charged groups.

One of possible confusion about the realistic features of our model is the common view that “with many parameters one can fit anything.” Such a view would be relevant if the parameters used were adjusted arbitrarily and could thus determine the results. As should be now clear from studies with force field and other related approaches,<sup>26</sup> it is entirely legitimate and useful to have potentials with many adjustable parameters as long as these parameters are fitted to properties that are not included in the specific modeling studies (e.g., studying the difference between enzymes to water reactions by a model that is not parameterized to reproduce these differences<sup>43</sup>). The same is true with respect to ionic radii in solvation models. Now the situation is similar with regards to our effective potential. Here the single-ion barrier and other features were determined from microscopic and semimacroscopic simulations that could not by themselves lead to arbitrary reproduction of the observed selectivity. Thus, the relevant question with regards to the parameters in the model is whether or not the changes that we allowed for some parameters were the reason for our apparent successes. The answer is no, since the sensitivity to changes in the parameters presented in Table II is relatively small in the range considered by us as a realistic range. Finally, we would like to clearly distinguish between the first step of our study (sets A–D in Table III), which involved no adjustment of parameter, and the second step, which examined the sensitivity to the nature of the free energy profile. Now, while the changes of the calculated profile in the second stage could reproduce any desirable result, it is very encouraging that the first step produced significant selectivity without adjusting the calculated profile.

Our studies pointed towards a strong sensitivity of the calculated profile to the dielectric constants used (in particular upon moving from a large value of  $\epsilon_{\text{eff}}$  to a small value, and in using small  $\epsilon_p$  without employing the LRA approach). Other workers and in particular Chung and Kuyucak<sup>17</sup> have reached a different conclusion. A part of the difference between the two views is due to the fact that very different models are being used. That is, Chung and Kuyucak<sup>17</sup> studied the energetics of ion channels by models that assume that the ion must be surrounded from all directions by water. Such models, which are perfectly valid for wide channels like porine, are not applicable to the narrow selectivity filters when the ion is practically inside the protein. This problem can be reduced by assuming artificially that the ion is surrounded by water, although in reality the water molecules cannot access the ion from the x and y direction. Now, with such an artificial salvation, the role of  $\epsilon_p$  is replaced by  $\epsilon_w$  and the results may be insensitive to  $\epsilon_p$ . At any rate, more consistent models that reflect experience from other proteins and can account for ion selectivity depend very strongly on the assumed  $\epsilon_p$ .

The importance of using a proper dielectric has been emphasized repeatedly in studies of globular proteins,<sup>27</sup> including membrane proteins,<sup>29</sup> but less so in the context

of ion channels. A case in point is the so-called helix dipole effect. A careful study<sup>44</sup> has demonstrated that the effect of the helix-macro-dipole is much smaller than what has been estimated using low dielectric models and that most of the effect is due to the localized dipoles at the last turn of the helix. Yet, a recent study<sup>45</sup> concluded that the effect of the main chain dipoles of distant helix residues is substantial. This study, however, used  $\epsilon = 2$  in a PB continuum model that does not reflect explicitly the protein reorganization. As explained elsewhere (e.g. Ref. 27) one has to use relatively large  $\epsilon_p$  models that do not involve an LRA reorganization procedure. Using a proper LRA procedure in the PDL/S-LRA approach gave a much smaller effect of the helix macro-dipole and distant residues. The difference between our approach to those that use low  $\epsilon$  in PB models is that we allow correctly for the protein reorganization. This reorganization, that was already considered in Åqvist et al.<sup>44</sup>, is one of the reasons why the effect of the helix dipole is small. Now a preliminary study in our lab established that the use of  $\epsilon = 2$  overestimates the effect of the helix dipole by a factor of 3 and that the effect is rather localized.

The present study examines the molecular origin of the selectivity of the KcsA channel. Taking the calculated free energy profiles at their face value underestimates the experimentally estimated selectivity. However, modest changes of these potentials (or the equivalent analytical potentials) lead to significant selectivity. In particular, about 2.0 kcal/mol increase in the entry and exit barriers for the  $\text{Na}^+$  ion can increase the selectivity to about 200–250. Similarly, increasing the binding energy of the  $\text{Na}^+$  ion (in the lowest energy site) by 1–2 kcal/mol can lead to the observed selectivity. It seems to us that these changes are at the limit of the error range of the calculations. Thus, studies that would focus on further quantification of the relative binding free energies of  $\text{K}^+$  and  $\text{Na}^+$  are clearly needed (see below).

It might be useful to comment at this point about the currently accepted model of concerted motion in the KcsA channel.<sup>5,16,46</sup> Such a motion is indeed observed in some of the  $\text{K}^+$  trajectories (Fig. 5). However, the degree of concertedness depends on the external potential and concentration. Apparently, even free energy profiles that would reproduce the observed population<sup>5</sup> might not lead to a completely concerted motion. It is clear that this issue requires further studies.

After considering the changes of the single ion profiles that lead to the observed selectivity, we examined other factors that can play an important role in discriminating between the  $\text{K}^+$  and  $\text{Na}^+$  channels. An interesting and potentially important factor is the difference in ion-ion interaction of the correlated motion of ion pairs (see also below). However, although this seems to be a real effect, regardless of its possible variation along the filter, the present study indicates that it is unlikely to be the major factor in controlling the KcsA selectivity. That is, even if the  $\text{Na}^+ \cdots \text{Na}^+$  interaction at the transition states of the concerted motion is larger than the  $\text{K}^+ \cdots \text{K}^+$  interaction, the difference in selectivity is not expected to increase by

more than a factor of 5. The reason is that the  $\text{Na}^+$  current will involve larger separation and more single ion trajectories, which will compensate for the larger interaction. Note in this respect that while our simulation conditions did not lead to concerted  $\text{Na}^+$  trajectories, the conclusions drawn from the  $\text{K}^+$  simulations with different  $\epsilon_{\text{eff}}$  should be applicable to cases where the  $\text{Na}^+$  trajectories are concerted. The issue of ion-ion interaction will be discussed further below.

It is still possible that a significant part of the selectivity might be due to the gate region. In the absence of definitive structural information on the open state of the gate (see discussion in Free Energy Profiles), we assumed here no barrier for both  $\text{K}^+$  and  $\text{Na}^+$  in this region. However, it is quite likely that the barrier for transfer through the gate region is somewhat different for  $\text{Na}^+$  than for  $\text{K}^+$ .

Although our free energy profiles do not account for the full observed selectivity, the calculated difference in the details of the  $\text{K}^+$  and  $\text{Na}^+$  profiles and the corresponding ion-ion interactions are quite instructive. These differences emerge from both the microscopic and semimacroscopic simulations and most probably reflect the reality in the KcsA channel. Although it is quite difficult to represent the complex difference between the  $\text{K}^+$ - $\text{K}^+$  and  $\text{Na}^+$ - $\text{Na}^+$  interaction by changing the corresponding  $\epsilon_{\text{eff}}$ , we clearly have here an effect that can be described as a change in the position dependent dielectric constant. At the loading states, the  $\text{Na}^+$  ion interacts more strongly with the channel dipoles (e.g., the carbonyls) and this makes it harder for these dipoles to compensate for the interaction with another ion and thus leads to a lower dielectric constant for ion-ion interaction. Unfortunately, this situation changes when the ions move to the transition states where it is harder to quantify it. Thus, at present we can only point out that it is essential to consider the change in ion-ion interaction in studies of ion selectivity. Of course, we also can (as was done here) examine the consequences of changes in the ion-ion interaction by changing the effective dielectric constant.

As should be obvious from the above discussion, we do not claim that we provided the final word about the origin of the selectivity of the KcsA channel. However, we provided a scheme that can be gradually refined by using directly and indirectly experimental information. First, we can gradually refine our free energy profiles and parameters. For example, we can try to reproduce the important information about the binding of  $\text{K}^+$  to  $\text{Ba}^{2+}$  blocked high-conductance  $\text{Ca}^{2+}$  activated  $\text{K}^+$  channel.<sup>47</sup> Reproducing this information and interpreting the corresponding experimental findings should help greatly in refining our approach. Second, even with the current uncertainty about the free energy profiles we are in a range that allows us to reproduce experimental information about current and selectivity while still satisfying the physical constraints on the system. We can, for example, find what modifications of the surfaces can lead to the observed selectivity and to other observed properties. This philosophy is similar in some respects to the current philosophy of Chung and coworkers<sup>31</sup> but with one significant difference. We strongly

believe that properly evaluated semimacroscopic free energy profiles should provide major constraints on the range of feasible phenomenological models.

In conclusion, we believe that further modeling studies along the line of the present work, coupled with an additional effort of obtaining more meaningful and stable results from microscopic simulations, should lead eventually to detailed understanding of the selectivity of the KcsA channel and related systems.

## ACKNOWLEDGMENTS

We are grateful to USC's high-performance computing center for computer time.

## REFERENCES

- Hille, B. Ionic channels of excitable membranes. 2nd ed. Sunderland, MA: Sinauer Assoc.; 1992.
- Eisenman G, Horn R. Ionic selectivity revisited: the role of kinetic and equilibrium processes in ion permeation through channels. *J Membr Biol* 1983;50:1025-1034.
- Latorre R, Miller C. Conduction and selectivity in potassium channels. *J Membr Biol* 1983;71:11-30.
- Doyle DA, Cabral JM, Pfuetzner RA, Kuo AL, Gulbis JM, Cohen SL, Chait BT, MacKinnon R. The structure of the potassium channel: Molecular basis of  $\text{K}^+$  conduction and selectivity. *Science* 1998;280:69-77.
- Morales-Cabral JH, Zhou Y, MacKinnon R. Energetic optimization of ion conduction rate by the  $\text{K}^+$  selectivity filter. *Nature* 2001;414:37-42.
- LeMasurier M, Heginbotham L, Miller C. J KcsA: it's a potassium channel. *J Gen Physiol* 2001;118:303-313.
- Cuello LG, Romero JG, Cortes DM, Perozo E. pH-dependent gating in the *Streptomyces lividans*  $\text{K}^+$  channel. *Biochemistry* 1998;37:3229-3236.
- Luzhkov V, Aqvist J.  $\text{K}^+/\text{Na}^+$  selectivity of the KcsA potassium channel from microscopic free energy perturbation calculations. *Biochim Biophys Acta* 2001;36446:1-9.
- Allen TW, Bliznyuk AA, Rendell AP, Kuyucak S, Chung S-H. The potassium channel: structure, selectivity and diffusion. *J Chem Phys* 2000;112:8191-8204.
- Shrivastava IH, Tieleman DP, Biggin PC, Sansom MSP.  $\text{K}^+$  versus  $\text{Na}^+$  ions in a K channel selectivity filter: a simulation study. *Biophys J* 2002;83:633-645.
- Nimigean CM, Miller C.  $\text{Na}^+$  block and permeation in a  $\text{K}^+$  channel of known structure. *J Gen Physiol* 2002;120:323-335.
- Jordan PC. Microscopic approaches to ion transport through transmembrane channels. The model system gramicidin. *J Phys Chem* 1987;91:6582-6591.
- Jordan PC. Ion-water and ion-polypeptide correlations in a gramicidin-like channel: a molecular dynamics study. *Biophys J* 1990;58:1133-1156.
- Aqvist J, Warshel A. Energetics of ion permeation through membrane channels. Solvation of  $\text{Na}^+$  by Gramicidin A. *Biophys J* 1989;56:171-182.
- Elber R, Chen DP, Eisenberg RD, Eisenberg R. Sodium in gramicidin: an example of a permion. *Biophys J* 1995;68:906-924.
- Aqvist J, Luzhkov V. Ion permeation mechanism of the potassium channel. *Nature* 2000;404:881-884.
- Chung SH, Kuyucak S. Ion channels: recent progress and prospects. *Eur J Biochem* 2002;31:283-293.
- Allen TW, Hoyles M, Kuyucak S, Chung SH. Molecular and Brownian dynamics study of ion selectivity and conductivity in the potassium channel. *Chem Phys Lett* 1999;313:358-365.
- Berneche S, Roux B. Energetics of ion conduction through the  $\text{K}^+$  channel. *Nature* 2001;414:73-77.
- Burykin A, Schutz CN, Villa J, Warshel A. Simulations of ion current in realistic models of ion channels: the KcsA potassium channel. *Proteins* 2002;47:265-280.
- Biggin PC, Smith GR, Shrivastava I, Choe S, Sansom MSP. Potassium and sodium ions in a potassium channel studied by molecular dynamics simulations. *Biochim Biophys Acta* 2001;1510:1-9.

22. Chung SH, Allen TW, Hoyles M, Kuyucak S. Permeation of ions across the potassium channel: Brownian dynamics studies. *Biophys J* 1999;77: 2517–2533.
23. Sham Y, Muegge I, Warshel A. Simulating proton translocations in proteins: Probing proton transfer pathways in the Rhodobacter Sphaeroides Reaction Center Proteins. 1999;36:484–500.
24. McQuarrie DA. *Statistical mechanics*. New York: Harper and Row; 1976.
25. Kubo R. The fluctuation-dissipation theorem. *Rept Progr Phys* 1966;29:255–284.
26. Warshel A. *Computer modeling of chemical reactions in enzymes and solutions*. New York: John Wiley & Sons; 1991.
27. Schutz CN, Warshel A. What are the dielectric “constants” of proteins and how to validate electrostatic models. *Proteins* 2001; 44:400–417.
28. Sham YY, Muegge I, Warshel A. The effect of protein relaxation on charge-charge interactions and dielectric constants of proteins. *Biophys J* 1998;74:1744–1753.
29. Johnson ET, Parson WW. Electrostatic interactions in an integral membrane protein. *Biochemistry* 2002;41:6483–6494.
30. Warshel A, Papazyan A. Electrostatic effects in macromolecules: fundamental concepts and practical modeling. *Curr Opin Struct Biol* 1998;8:211–217.
31. Edwards S, Corry B, Kuyucak S, Chung S-H. Continuum electrostatics fails to describe ion permeation in the gramicidin channel. *Biophys J* 2002;83:1348–1360.
32. Smart OS, Neduvellil JG, Wang X, Wallace BA, Sansom MSP. HOLE: a program for the analysis of the pore dimensions of ion channel structural models. *J Mol Graph* 1996;14:354–360.
33. Smith GR, Sansom MSP. Effective diffusion coefficient of  $K^+$  and  $Cl^-$  ions in ion channel models. *Biophys Chem* 1999;79:129–151.
34. Wang MC, Uhlenbeck GE. On the theory of the Brownian motion II. *Rev Mod Phys* 1945;17:323–342.
35. Kato M, Lee FS, Eisenman G, Warshel A., manuscript in preparation.
36. Lee FS, Chu ZT, Warshel A. Microscopic and semimicroscopic calculations of electrostatic energies in proteins by the POLARIS and ENZYMIK programs. *J Comp Chem* 1993;14:161–185.
37. Åqvist, J. Ion-water interaction potentials derived from free energy perturbation simulations. *J Chem Phys* 1990;94:8021–8024.
38. Tissandier MD, Cowen KA, Feng WY, Gundlach E, Cohen MH, Earhart AD, Coe JV. The proton’s absolute aqueous enthalpy and Gibbs free energy of solvation from cluster-ion solvation data. *J Phys Chem* 1998;102:7787–7794.
39. King G, Warshel A. A surface constrained all-atom solvent model for effective simulations of polar solutions. *J Chem Phys* 1989;91: 3647–3661.
40. Lee FS, Warshel A. A local reaction field method for fast evaluation of long-range electrostatic interactions in molecular simulations. *J Chem Phys* 1992;97:3100–3107.
41. Perozo E, Cortes DM, Cuello LG. Structural rearrangements underlying  $K^+$ -channel activation gating. *Science* 1999;285:73–78.
42. Gullingsrud JR, Braun R, Schulten K. Reconstructing potentials of mean force through time series analysis of steered molecular dynamics simulations. *J Comput Chem* 1999;151:190–211.
43. Åqvist J, Warshel A. Simulation of enzyme reactions using valence bond force fields and other hybrid quantum/classical approaches. *Chem Rev* 1993;93:2523–2544.
44. Åqvist J, Luecke H, Quijcho FA, Warshel A. Dipoles localized at helix termini of proteins stabilize charges. *Proc Natl Acad Sci* 1991;88:2026.
45. Roux B, Berneche S, Im W. Ion channels, permeation and electrostatics: insight into the function of KcsA. *Biochemistry* 2000;39: 13295–13306.
46. Miller C. See potassium run. *Nature* 2000;414:23–24.
47. Neyton J, Miller C. Discrete  $Ba^{2+}$  block as a probe of ion occupancy and pore structure in the high-conductance  $Ca^{2+}$ -activated  $K^+$  channel. *J Gen Physiol* 1988;92:569–586.